Depth dependent modification of optical constants arising from H^+ implantation in n-type 4H-SiC measured using coherent acoustic phonons

Andrey Baydin, Halina Krzyzanowska, Munthala Dhanunjaya, S. V. S. Nageswara Rao, Jimmy L. Davidson, Leonard C. Feldman, and Norman H. Tolk

Citation: APL Photonics **1**, 036102 (2016); doi: 10.1063/1.4945443
View online: http://dx.doi.org/10.1063/1.4945443
View Table of Contents: http://aip.scitation.org/toc/app/1/3
Published by the American Institute of Physics

APL PHOTONICS **1**, 036102 (2016)

Depth dependent modification of optical constants arising from H^+ implantation in n-type 4H-SiC measured using coherent acoustic phonons

Andrey Baydin,[1,a] Halina Krzyzanowska,[1,2] Munthala Dhanunjaya,[3] S. V. S. Nageswara Rao,[3] Jimmy L. Davidson,[4] Leonard C. Feldman,[1,5] and Norman H. Tolk[1]

[1]*Department of Physics and Astronomy, Vanderbilt University, Nashville, Tennessee 37235, USA*
[2]*Maria Curie-Sklodowska University, Pl. M. Cuire-Sklodowskiej 1, 20-031 Lublin, Poland*
[3]*School of Physics, University of Hyderabad, Hyderabad 500046, India*
[4]*Electrical Engineering and Computer Sciences, Vanderbilt University, Nashville, Tennessee 37235, USA*
[5]*Institute of Advanced Materials, Devices, and Nanotechnology, Rutgers University, New Brunswick, New Jersey 08901, USA*

(Received 23 December 2015; accepted 24 March 2016; published online 6 June 2016)

Silicon carbide (SiC) is a promising material for new generation electronics including high power/high temperature devices and advanced optical applications such as room temperature spintronics and quantum computing. Both types of applications require the control of defects particularly those created by ion bombardment. In this work, modification of optical constants of 4H-SiC due to hydrogen implantation at 180 keV and at fluences ranging from 10^{14} to 10^{16} cm^{-2} is reported. The depth dependence of the modified optical constants was extracted from coherent acoustic phonon spectra. Implanted spectra show a strong dependence of the 4H-SiC complex refractive index depth profile on H^+ fluence. These studies provide basic insight into the dependence of optical properties of 4H silicon carbide on defect densities created by ion implantation, which is of relevance to the fabrication of SiC-based photonic and optoelectronic devices. [http://dx.doi.org/10.1063/1.4945443]

Silicon carbide (SiC) is a wide band gap semiconductor, ideally suited to high power, high temperature, and high frequency electronic device applications. Recent progress in materials structure and interface passivation has allowed the creation of a useful SiC MOS technology.[1] More recently, it has been recognized that isolated defects in SiC can serve as long-lifetime atomic like states suitable for coherent single photon generation and possibly quantum computing structures.[2–4] Thus, defect creation and defect annealing are important processes associated with these burgeoning SiC technologies.

In this letter, we report depth dependent modification of the optical constants of n-type 4H-SiC due to defect creation by hydrogen implantation at 180 keV. Optical constants are obtained using coherent acoustic phonon (CAP) spectroscopy. Such knowledge is essential for reliable fabrication of future photonic/optoelectronic devices using silicon carbide. Proton irradiation in space is well known to be responsible for the degradation of satellite's on-board electronics due to radiation damage. Thus, the understanding of the damage (vacancies, interstitials, and their related defects) created by hydrogen implantation is crucial for designing reliable devices for use in space. Hydrogen related defects have been studied for the past decade by electrical techniques (DLTS).[5–8] Depth dependent structural damage was probed by RBS and hydrogen profiles by SIMS[9,10] at

[a]Author to whom correspondence should be addressed. Electronic mail: andrey.baydin@vanderbilt.edu

implantation fluences above 10^{16} cm^{-2} which defines the sensitivity limits of these techniques. Here, the CAP technique is shown to be two orders of magnitude more sensitive than the channeling probe which is consistent with a previous study.[11] To the best of our knowledge, this is the first time that the CAP technique has been applied to obtain a depth dependent complex refractive index.

We used Si-face n-type 4H-SiC (ρ = 0.7 Ω·cm) 10 μm epilayers grown on 4H-SiC substrate by a CVD process. Following fabrication, they were implanted at room temperature with 180 keV hydrogen ions with fluences ranging from 10^{14} to 10^{16} cm^{-2} at 0.9 μA current. No annealing has been carried out following implantation.

CAP spectroscopy, also known as picosecond ultrasonics, is a pump probe technique. When an ultrafast high-intensity pump pulse hits an absorbing material, it excites electrons that decay into optical and then longitudinal acoustic phonons, which subsequently traverse the material. The CAP wave may be thought of as a crystal strain wave travelling into the solid at the speed of sound. To generate high amplitude coherent acoustic phonons, a thin metal film is typically deposited onto the material surface. Creation of CAP waves can be classically explained by thermal expansion of a metal transducer[12] and the transfer of the elastic wave to the substrate. A delayed probe beam is then reflected both from the surface of the material and from the traveling CAP wave, giving rise to an oscillatory response due to interference between the two reflected beams as shown in Fig. 1. Using this approach, damaged regions at particular depths in the specimen result in a decrease in the signal amplitude and a phase shift in the oscillatory CAP signal with respect to CAP response of the unimplanted specimen. The depth resolution is estimated to be approximately 40 nm based on the CAP wave and probe light pulse widths.

In previous studies, quantitative defect profiles in He implanted GaAs[13] and also the optical damage cross section surrounding 400 keV Ne^{++}-ion tracks in GaAs were experimentally determined with high sensitivity.[11] In addition, research on ion-implanted diamond revealed a fluence-dependent decrease in the real and increase in the imaginary parts of the refractive index as well as a sign reversal in the photoelastic coefficient.[14,15]

In the present experiments, a 10 nm aluminum layer was used as a transducer, deposited using an Angstrom resistive evaporator. CAP measurements were taken using a Coherent Mira 900 Ti:sapphire laser producing 150-fs pulses at 76 MHz. The pump beam was tuned to 800 nm with 230 mW power and the probe beam was frequency-doubled to 400 nm using Beta Barium

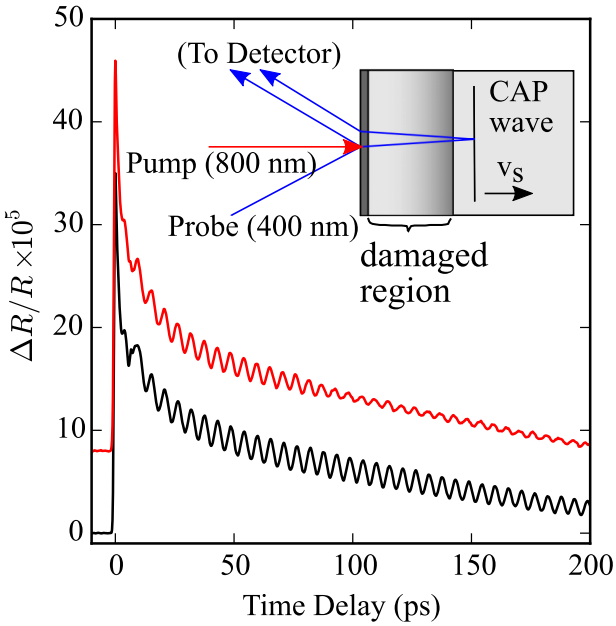

FIG. 1. Typical CAP responses for implanted (red) at 1×10^{16} cm^{-2} fluence and unimplanted (black) n-type 4H-SiC, vertically offset for clarity. *Inset*: CAP experiment configuration showing strain-wave induced self-interference in the probe reflectivity.

Borate (BaB_2O_4), a nonlinear optical crystal with 2 mW power. Both beams were focused onto the specimen with spot diameters of 100 μm and 90 μm for pump and probe, respectively. The pump beam was chopped using an optical chopper at about 3 kHz. The typical pump-probe reflectivity response for both unimplanted and implanted at 10^{16} cm^{-2} fluence specimens is shown in Fig. 1. Oscillations arising from the traveling CAP wave are superimposed on the thermal response of metal electrons. In the following analysis, the thermal response has been subtracted out, leaving only the CAP oscillations.

The oscillatory part of the reflectivity response measured in CAP spectroscopy can be characterized as[12,16]

$$\frac{\Delta R(t)}{R_0} \propto A \sin\left(\frac{2\pi t}{T} + \phi\right) e^{-\frac{t}{\tau}}, \tag{1}$$

where t is the time, T is the period, τ is the damping time, and ϕ is the phase. As the CAP wave travels with the speed of sound, the time t can be related to the depth z in the material by the equation $z = v_s t$. The oscillation amplitude A is related to the derivatives of real and imaginary parts of the complex refractive index $N = n + i\kappa$ with respect to the strain η as follows:

$$A \propto \sqrt{\left(\frac{\partial n}{\partial \eta}\right)^2 + \left(\frac{\partial \kappa}{\partial \eta}\right)^2}. \tag{2}$$

The period of the oscillation T depends on the real part of refractive index n, speed of sound (CAP wave) v_s, wavelength λ, and angle of incidence θ of the probe beam as follows:

$$T = \frac{\lambda}{2nv_s \cos\theta}. \tag{3}$$

The damping time τ is proportional to penetration depth of the probe beam and, consequently, extinction coefficient κ,

$$\tau = \frac{\lambda}{4\pi\kappa v_s \cos\theta}. \tag{4}$$

The measured period and damping time of the CAP oscillations for unimplanted specimen are $T = 5.584$ ps and $\tau = 223.8$ ps, respectively. Using these parameters, we calculate n and κ from formulae (3) and (4) with $\theta = 27°$, $v_s = 13.1$ nm/ps, and $\lambda = 400$ nm to be $n = 3.07$ and $\kappa = 0.0122$. These values are in good agreement with previously reported values.[17]

Fig. 2 shows CAP oscillations for specimens implanted at fluences of 10^{14}, 10^{15}, and 10^{16} cm^{-2}. Spectra for the implanted specimens are plotted on top of the spectra for the unimplanted specimen. The lattice damage resulting from ion implantation is shown on the top of Fig. 2. It is estimated from Monte Carlo simulations performed using the transport of ions in matter (TRIM) code.[18]

There is no detectable defect related modification of the CAP signal at 10^{14} cm^{-2} fluence. This defines the sensitivity limit of the CAP technique at this wavelength to H^+ induced optical damage. Two important features of the data are noted for higher implantation fluences. As the implantation fluence increases, the amplitude of the CAP oscillations decreases. This observation is related to the increased absorption of the probe light as expressed in the imaginary part of the complex refractive index arising from the structural damage caused by the hydrogen implantation. Insets in Fig. 2 show phase shifts of the CAP oscillations in the implanted specimens to the left on the time scale with respect to those in the unimplanted specimens. This can be attributed to an increase in the real part of the complex refractive index of the implanted specimens that results in an increased optical path length for the probe pulse as it travels to the CAP wave and back through damaged SiC lattice as discussed below.

As can be seen from Equations (1)-(4), the CAP oscillatory response primarily depends on the quantities $n, \kappa, \partial n/\partial\eta, \partial\kappa/\partial\eta$. For perfect single crystals, these values are constant as a function of depth. However, ion implantation induces a spatially varying lattice damage profile, which is dependent on depth. The reduction in the oscillatory amplitudes related to the depth dependent implantation damage in SiC lattice may be attributed to (a) modification of the extinction coefficient induced by the lattice defects and/or (b) changes in the derivative terms $\partial(n,k)/\partial\eta$. Fig. 2 shows an overall

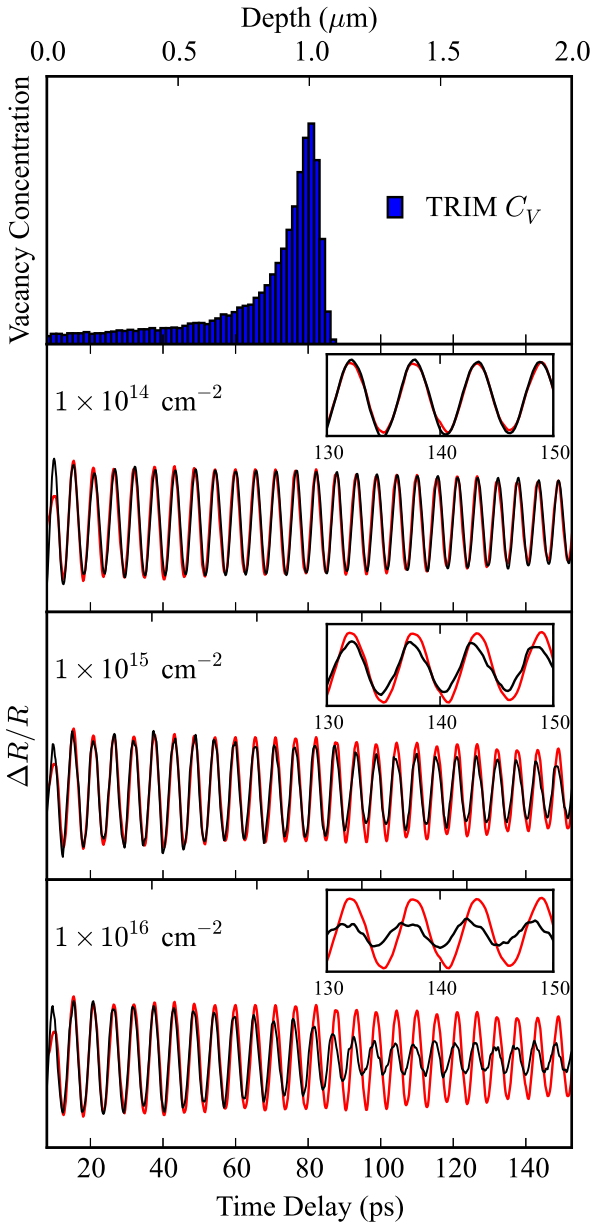

FIG. 2. CAP oscillations in the pump-probe reflectivity signal of ion-implanted SiC specimens at multiple fluences (black lines). The red line behind each curve is the corresponding response for an unimplanted specimen. Above the CAP responses are the damage-induced vacancy distribution as calculated by the TRIM code. The insets show spectra on the smaller scale to indicate phase shift between two curves.

cumulative decrease in the amplitude beyond the damaged region that indicates a damage-induced modification of the extinction coefficient. Therefore, in this work, we make an assumption that the derivative terms $\partial(n,k)/\partial\eta$ are constant with respect to the depth in the implanted specimens, i.e., do not contribute to the modulation of the amplitude.

In order to obtain changes in the extinction coefficient $\Delta\kappa$ due to the hydrogen implantation, we divide the envelope of oscillatory signal $\Delta R(z)/R$ corresponding to unimplanted specimen by the envelope of oscillatory signal $\Delta R'(z)/R'$ corresponding to implanted specimen (see Fig. 3(a)) using formulae (1) and (4), and after taking the natural logarithm of both sides of the equation, we have

$$\ln\left(\frac{\Delta R(z)/R}{\Delta R'(z)/R'}\right) = \frac{4\pi\cos\theta}{\lambda}\int_0^z \Delta\kappa(z')\,dz'. \tag{5}$$

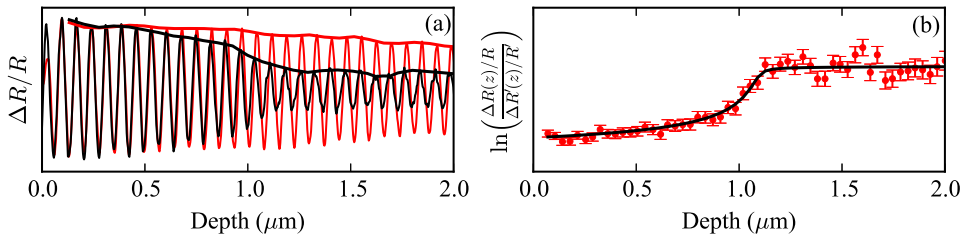

FIG. 3. (a) CAP data obtained at a fluence of 10^{16} contrasting the implanted/unimplanted data. (b) Fit of the implanted/unimplanted experimental data using Equation (5).

By assuming that $\Delta\kappa$ behaves as a Pearson IV function, which is commonly used to describe ion-implanted distributions, we fit the parameters of Pearson IV function in Equation (5) to the experimental data (see Fig. 3(b)).

Fig. 4 shows changes in the extinction coefficient $\Delta\kappa(z)$ arising from the 180 keV hydrogen implantation in n-type 4H-SiC at different fluences. Clearly, changes in the extinction coefficient are proportional to the defect densities as estimated by TRIM code. The magnitude of these changes decreases as the implantation fluence decreases. The red curve corresponding to the relatively small fluence of 3×10^{14} cm^{-2} is broadened and shifted due to noise in the CAP spectrum.

It is assumed in this study that the longitudinal speed of sound in the implanted specimens of 4H-SiC is largely unaffected by the implantation induced damage of the lattice. This assumption is supported by the fact that the speed of sound in an amorphous material is shown to be somewhat smaller than that in the same type of crystalline material.[19,20] Thus, a substantial slowing of the speed of sound would result in a phase shift of CAP spectra of the implanted specimen to the right with respect to the spectra of the unimplanted specimen. However, we observe a phase shift in the opposite direction. For this reason, we attribute the observation of the phase shift primarily to an increase in the real part of the refractive index. Thus, the phase shift $\Delta\psi$ between the unimplanted

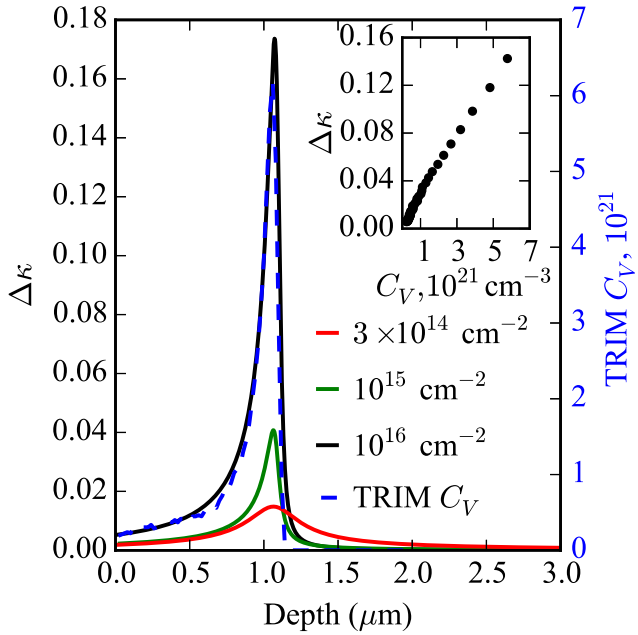

FIG. 4. Observed changes in the extinction coefficient as a function of depth using CAP, following hydrogen implantation. Dashed line represents TRIM vacancy profile for the highest fluence of the implantation. The inset shows the implantation induced extinction coefficient change versus vacancy concentration calculated from TRIM. The red curve corresponding to the relatively small fluence of 3×10^{14} cm^{-2} is broadened and shifted due to the noise in the CAP spectrum.

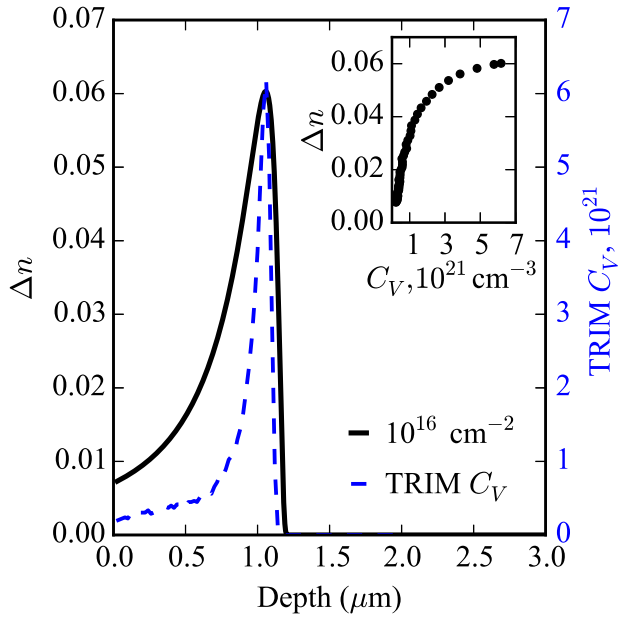

FIG. 5. Observed changes in the refractive index as a function of depth using CAP, following hydrogen implantation. The dashed line represents the TRIM vacancy profile for the highest implantation fluence, 10^{16} cm^{-2}. The inset shows the implantation induced refractive index change versus vacancy concentration calculated from TRIM.

and implanted spectra can be determined as

$$\Delta\psi = \frac{4\pi\cos\theta}{\lambda}\left[\int_0^z \Delta n\,(z')\,dz'\right]. \tag{6}$$

Again, assuming that the change in the real part of the complex refractive index Δn due to the hydrogen implantation behaves as a Pearson IV function, we fit Equation (6) to the experimental data to obtain depth dependent profiles of the real refractive index change Δn as shown in Fig. 5. Here, the phase shift was measurable only for the highest dose of implantation.

The implantation-induced change in the real part of the complex refractive index profile is broader and skewed more to the surface side than the vacancy/defect profile calculated by TRIM code. This indicates a nonlinear dependence of modified refractive index on vacancy/defect concentration. The dependence is linear up to a vacancy concentration of about 10^{21} cm^{-3}. In other words, when distances between vacancies are smaller than 10 Å (about lattice constant along c-axis), changes in the real part of the complex refractive index due to hydrogen implantation tend to saturate. In comparison, the increase in the real part of the complex refractive index in boron implanted CVD type IIa diamond deviates from linear dependence for vacancy concentrations above 2×10^{21} cm^{-3}.[21]

There have been previous studies of damage arising from ion implantation leading to changes in the refractive index in a variety of optical materials. It was observed for many of those materials that changes in the refractive index Δn arise mostly from changes in local volume ΔV.[22] However, there are other defect-dependent parameters that can contribute to refractive index change such as the atomic bond polarizability α and the structure factor F. These factors are embodied in the Wei adaptation of the Lorentz-Lorenz equation[23–25]

$$\frac{\Delta n}{n} = \frac{(n^2-1)(n^2+2)}{6n^2}\left[-\frac{\Delta V}{V}+\frac{\Delta\alpha}{\alpha}+F\right]. \tag{7}$$

For the case of silicon carbide, volume expansion of the damaged region was observed,[26,27] which if treated as the only factor would result in a decrease in the refractive index. However, in the present work, an increase in n and κ was observed as the defect concentration increases. We

postulate that the observed increase in the refractive index n is due to contributions from the atomic bond polarizability α and/or structure factor F. Thus, ionization from electronic stopping is likely to be a major contributing factor leading to an increase in the real part of the complex refractive index. Further work is needed to determine the relative contributions of these and possibly other parameters.

It is interesting to compare these results to the studies of the index change with ion bombardment in similar covalently bonded materials. For example, several studies report increased refractive index arising from ion implantation in diamond,[21,28–31] silicon,[32–35] and germanium,[36] despite considerable volume expansion. In all cases, the increase is attributed to a change in the atomic bond polarizability. Thus, this new report of the change in index with ion bombardment adds one more significant point to the body of data that relate the large change in polarizability with ion bombardment for covalent semiconductors.

In conclusion, we have measured depth-dependent profiles of optical constants arising from hydrogen ion implantation at low doses in n-type 4H-SiC using coherent acoustic phonon spectroscopy. CAP spectroscopy is shown to be a sensitive non-destructive tool for studying the implantation damage-induced modification of the opto-electronic nature of silicon carbide lattice. Our results show a strong dependence of the 4H-SiC complex refractive index as a function of depth and H^+ fluence. We note also that the implantation-modified refractive index (real part) profile is broader and skewed toward the surface as compared to that of the implantation induced structural damage profile, predicted by Monte Carlo calculations. This increase in the real part of the refractive index may be accounted for by invoking changes in the atomic bond polarizability arising from ionization due to electronic stopping during implantation. Both real and imaginary parts of the complex refractive index are observed to increase as a function of defect density. These studies provide insight into the influence of defects on optical properties of relevance to the fabrication of SiC-based waveguides and other photonic and optoelectronic devices.

The authors would like to gratefully acknowledge the ARO for financial support under Contract No. W911NF-14-1-0290. Portions of this work were completed using the shared resources of the Vanderbilt Institute of Nanoscale Science and Engineering (VINSE) core laboratories. We also would like to thank LEIB, IUAC, New Delhi, India for the beam time.

[1] S. Dhar, S. Wang, J. R. Williams, S. T. Pantelides, and L. C. Feldman, MRS Bull. **30**, 288 (2005).
[2] D. J. Christle, A. L. Falk, P. Andrich, P. V. Klimov, J. U. Hassan, N. T. Son, E. Janzén, T. Ohshima, and D. D. Awschalom, Nat. Mater. **14**, 160 (2014).
[3] M. Widmann, S.-Y. Lee, T. Rendler, N. T. Son, H. Fedder, S. Paik, L.-P. Yang, N. Zhao, S. Yang, I. Booker, A. Denisenko, M. Jamali, S. A. Momenzadeh, I. Gerhardt, T. Ohshima, A. Gali, E. Janzén, and J. Wrachtrup, Nat. Mater. **14**, 164 (2014).
[4] S. Castelletto, B. C. Johnson, V. Ivády, N. Stavrias, T. Umeda, A. Gali, and T. Ohshima, Nat. Mater. **13**, 151–156 (2014).
[5] M. S. Janson, M. K. Linnarsson, A. Hallen, B. G. Svensson, N. Achtziger, L. Uneus, A. Lloyd spetz, and U. Forsberg, Phys. Scr. **2004**, 99.
[6] G. Alfieri, E. V. Monakhov, B. G. Svensson, and A. Hallén, J. Appl. Phys. **98**, 113524 (2005).
[7] G. Alfieri and T. Kimoto, J. Appl. Phys. **101**, 103716 (2007).
[8] G. Alfieri and T. Kimoto, New J. Phys. **10**, 073017 (2008).
[9] A. Barcz, M. Kozubal, R. Jakieła, J. Ratajczak, J. Dyczewski, K. Gołaszewska, T. Wojciechowski, and G. K. Celler, J. Appl. Phys. **115**, 223710 (2014).
[10] V. P. Amarasinghe, L. Wielunski, A. Barcz, L. C. Feldman, and G. K. Celler, ECS J. Solid State Sci. Technol. **3**, P37 (2014).
[11] A. Steigerwald, A. B. Hmelo, K. Varga, L. C. Feldman, and N. Tolk, J. Appl. Phys. **112**, 013514 (2012).
[12] C. Thomsen, H. T. Grahn, H. J. Maris, and J. Tauc, Phys. Rev. B **34**, 4129 (1986).
[13] A. Steigerwald, Y. Xu, J. Qi, J. Gregory, X. Liu, J. K. Furdyna, K. Varga, A. B. Hmelo, G. Lüpke, L. C. Feldman, N. Tolk, G. Lüpke, L. C. Feldman, and N. Tolk, Appl. Phys. Lett. **94**, 1 (2009).
[14] J. Gregory, A. Steigerwald, H. Takahashi, A. Hmelo, and N. Tolk, Appl. Phys. Lett. **101**, 181904 (2012).
[15] J. Gregory, A. Steigerwald, H. Takahashi, A. Hmelo, and N. Tolk, Appl. Phys. Lett. **103**, 049904 (2013).
[16] S. Wu, P. Geiser, J. Jun, J. Karpinski, and R. Sobolewski, Phys. Rev. B **76**, 085210 (2007).
[17] R. Ahuja, A. Ferreira Da Silva, C. Persson, J. M. Osorio-Guillén, I. Pepe, K. Järrendahl, O. P. A. Lindquist, N. V. Edwards, Q. Wahab, and B. Johansson, J. Appl. Phys. **91**, 2099 (2002).
[18] J. F. Ziegler, M. D. Ziegler, and J. P. Biersack, Nucl. Instrum. Methods Phys. Res., Sect. B **268**, 1818 (2010).
[19] D. B. Hondongwa, L. R. Olasov, B. C. Daly, S. W. King, and J. Bielefeld, Thin Solid Films **519**, 7895 (2011).
[20] I. R. Cox-Smith, J. Vac. Sci. Technol., A **3**, 674 (1985).
[21] A. Battiato, F. Bosia, S. Ferrari, P. Olivero, A. Sytchkova, and E. Vittone, Opt. Lett. **37**, 671 (2012).
[22] P. D. Townsend, P. J. Chandler, and L. Zhang, *Optical Effects of Ion Implantation* (Cambridge University Press, 2006).
[23] D. T. Y. Wei, Appl. Phys. Lett. **25**, 329 (1974).
[24] K. Wenzlik, J. Heibei, and E. Voges, Phys. Status Solidi A **61**, K207 (1980).

[25] T. C. Sum, A. A. Bettiol, J. A. van Kan, S. Venugopal Rao, F. Watt, K. Liu, and E. Y. B. Pun, J. Appl. Phys. **98**, 033533 (2005).
[26] I. T. Bae, W. J. Weber, and Y. Zhang, J. Appl. Phys. **106**, 123525 (2009).
[27] W. Jiang, C. M. Wang, W. J. Weber, M. H. Engelhard, and L. V. Saraf, J. Appl. Phys. **95**, 4687 (2004).
[28] R. L. Hines, Phys. Rev. **138**, A1747 (1965).
[29] P. Olivero, S. Calusi, L. Giuntini, S. Lagomarsino, A. Lo Giudice, M. Massi, S. Sciortino, M. Vannoni, and E. Vittone, Diamond Relat. Mater. **19**, 428 (2010).
[30] M. A. Draganski, E. Finkman, B. C. Gibson, B. A. Fairchild, K. Ganesan, N. Nabatova-Gabain, S. Tomljenovic-Hanic, A. D. Greentree, and S. Prawer, Opt. Mater. Express **2**, 644 (2012).
[31] S. Lagomarsino, P. Olivero, S. Calusi, D. G. Monticone, L. Giuntini, M. Massi, S. Sciortino, A. Sytchkova, A. Sordini, and M. Vannoni, Opt. Express **20**, 19382 (2012).
[32] G. K. Hubler, C. N. Waddell, W. G. Spitzer, J. E. Fredrickson, S. Prussin, and R. G. Wilson, J. Appl. Phys. **50**, 3294 (1979).
[33] G. K. Hubler, P. R. Malmberg, C. A. Carosella, T. P. Smith, W. G. Spitzer, C. N. Waddell, and C. N. Phillippi, Radiat. Eff. **48**, 81 (1980).
[34] C. N. Waddell, J. Appl. Phys. **53**, 5851 (1982).
[35] J. E. Fredrickson, Appl. Phys. Lett. **40**, 172 (1982).
[36] K.-W. Wang, W. G. Spitzer, G. K. Hubler, and E. P. Donovan, J. Appl. Phys. **57**, 2739 (1985).